Chemical Engineering Journal 117 (2006) 143–154

Chemical Engineering Journal

www.elsevier.com/locate/cej

# A diffusional analysis for the oxidation on a plane metal–oxide interface

Eun-Suok Oh*

*Department of Aerospace Engineering, Texas A&M University College Station, TX 77843-3141, USA*

Received 15 March 2005; accepted 30 December 2005

**Abstract**

Based on the diffusion of oxygen, the oxidation on a plane metal–oxide interface is analyzed using a perturbation scheme. Unlike previous models, the reaction rate and the oxygen dissolution into metal are taken into account. One-dimensional Landau transformation is applied to transform a moving domain by volumetric expansion during oxidation into a fixed domain. We investigate how the oxide thickness depends on the reaction rate, the ratio of diffusion coefficients, the molar density ratio, etc. By comparison of the results with the experimental observations, we compute the diffusion coefficients of oxygen in the metal and oxide, as well as the reaction rate coefficient for silicon and titanium oxidation.


*Keywords:* Diffusion; Oxidation; Metal–oxide interface; Perturbation analysis; Landau transformation

## 1. Introduction

The oxidation of metals has been extensively studied since its important roles in modern technology [1–6]. The oxidation of silicon is one of the critical steps in the fabrication of semiconductor devices to make a barrier to dopant diffusion into the substrate. The application of metal matrix composites (MMC) has been increased and the life of them may be significantly reduced by the oxidation at high temperatures.

For a class of oxidation such as silicon or titanium oxidation, oxygen diffuses through the oxide and reacts with the metal at the metal–oxide interface. Part of the oxygen diffusing the oxide dissolves into the metal [7,8]. There occurs volumetric expansion during the oxidation, because the density of the oxide is typically less than that of the metal. This volumetric expansion can be characterized by the Pilling–Bedworth ratio [9], which is the molar density ratio of the metal to the oxide. Due to this volumetric expansion, both the metal–oxide interface and the oxide–oxygen (air) interface move and thus the oxidation is thought as a non-linear moving-boundary value problem [10,11].

A classical model on the oxidation has been proposed by Wagner [1]. It was assumed that diffusion through the oxide is the rate determining step during the oxidation process, that no oxygen dissolves into metal, and that thermodynamic equilibrium is established at both the oxide–oxygen interface and the metal–oxide interface. Consequently, a parabolic rate of the oxide growth was obtained. Several authors [2–4] considered oxygen diffusion into the metal. The oxygen concentration was assumed to be linearly distributed within the oxide, but this leads the solution to be valid only for a stationary interface [12]. Without this assumption, Lagoudas et al. [12] have calculated the oxygen concentrations in both the metal and the oxide. In their model, however, the volumetric expansion during oxidation was not taken into account.

In this paper, we will develop a solution by a perturbation analysis for the oxidation of a metal on a plane metal–oxide interface without any limitations mentioned above. Once the moving boundaries by the oxidation are immobilized by the Landau transformations [13], a regular perturbation technique is employed [14,15]. Here the perturbation parameter $\phi$ is the ratio of the molar density

* Corresponding author at: LG Chem/Research Park, 104-1 Moonji-dong Yuseong-gu, Daejeon 305-860, South Korea. Tel.: +82 42 870 6076; fax: +82 42 862 6072.

*E-mail address:* eunsuokoh@gmail.com.

1385-8947/$ – see front matter © 2006 Elsevier B.V. All rights reserved.
doi:10.1016/j.cej.2005.12.018

**Nomenclature**

| | |
|---|---|
| $c_{(A)}^{(B)}$ | concentration of $A$ in phase B |
| $c_{eq}$ | equilibrium concentration of oxygen at the oxide–oxygen interface |
| $\mathcal{D}^{(B)}$ | diffusion coefficient of oxygen in phase B |
| $k$ | reaction rate coefficient for the oxidation |
| $N_{(O_2)}^{(B)}$ | molar flux of oxygen in phase B |
| $r_{(A)}^{(\sigma)}$ | rate of production of species $A$ |
| $u$ | speed of displacement of the metal–oxide interface |
| $v_{(A)}^{(B)}$ | velocity of $A$ in phase B |

*Greek letters*

| | |
|---|---|
| $\alpha$ | ratio of the diffusion coefficient of oxygen in metal to that in oxide |
| $\gamma$ | Pilling–Bedworth ratio |
| $\phi$ | perturbation parameter |
| $\boldsymbol{\xi}$ | unit normal to the phase interface |
| $\chi$ | variable for new coordinate systems |

of oxygen at the oxide–oxygen interface to the molar density of the metal. We will first investigate how the oxide thickness depends on the reaction rate, the ratio of diffusion coefficients, the molar density ratio, etc., and then determine the diffusion coefficients for oxygen in the metal and oxide, and the reaction rate coefficient at the metal–oxide interface for the oxidation of silicon and titanium.

## 2. Problem statement

As shown in Fig. 1, a solid initially composed of pure metal is exposed to an oxygen environment. The following assumptions will be made to model the oxidation of the metal.

(i) The frame of reference is chosen such that the oxide is stationary.
(ii) The metal is initially oxygen-free.
(iii) Equilibrium is established at the oxide–oxygen interface.
(iv) The molar density of metal $c_{(met)}$ and the molar density of oxide $c_{(ox)}$ are independent of position and time.
(v) Temperature is independent of position and time, which means that the energy released by the reaction is dissipated rapidly.
(vi) Oxygen diffuses through the oxide to react with the metal to form the oxide at the metal–oxide interface. The oxidation is a simple first-order reaction with respect to oxygen.
(vii) All physical parameters are considered to be constants.

## 3. Oxidation of metals

The growth of oxide on a planar surface is based on the diffusion of oxygen from air or oxygen environment to the metal surface, where the oxidation of metal proceeds to form a fresh oxide.

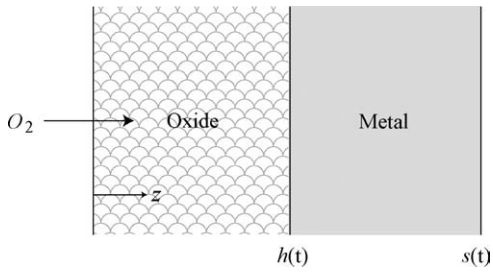


Fig. 1. Schematic of the oxidation on a 1-D planar surface.

The differential mass balances [16] for $O_2$ in an oxide and its metal layer are

$$\frac{\partial c^{(o)}_{(O_2)}}{\partial t} + \frac{\partial N^{(o)}_{(O_2)}}{\partial z} = 0, \quad 0 < z < h(t) \tag{1}$$

$$\frac{\partial c^{(m)}_{(O_2)}}{\partial t} + \frac{\partial N^{(m)}_{(O_2)}}{\partial z} = 0, \quad h(t) < z < s(t) \tag{2}$$

In what follows, superscripts (m) and (o) refer to the metal and the oxide layer, and subscripts refer to components; $c_{(O_2)}$ and $N_{(O_2)}$ are the concentration of oxygen and the molar flux of oxygen. The molar flux of species $A$ is defined as

$$N_{(A)} \equiv c_{(A)} v_{(A)} \tag{3}$$

in which $v_{(O_2)}$ is the $z$ component of velocity of oxygen.

Fick's first law [16] of one-dimensional binary diffusion has a form

$$N_{(A)} = x_{(A)}(N_{(A)} + N_{(B)}) - c\,\mathcal{D}_{(AB)} \frac{\partial x_{(A)}}{\partial z} \tag{4}$$

where $x_{(A)}$ is the mole fraction of component $A$ and $\mathcal{D}_{(AB)}$ is the diffusion coefficient of $A$ in $B$. Since $x_{(A)} = c_{(A)}/c$, Eq. (4) becomes

$$N_{(A)} = \frac{c_{(A)}}{c - c_{(A)}} N_{(B)} - \frac{c^2}{c - c_{(A)}} \mathcal{D}_{(AB)} \frac{\partial}{\partial z}\left(\frac{c_{(A)}}{c}\right) = \frac{c_{(A)}}{c_{(B)}} N_{(B)} - \mathcal{D}_{(AB)} \frac{\partial c_{(A)}}{\partial z} + \mathcal{D}_{(AB)} \frac{c_{(A)}}{c_{(B)}} \frac{\partial c_{(B)}}{\partial z} \tag{5}$$

From the definition of the molar flux (3), this finally becomes

$$N_{(A)} = c_{(A)} v_{(B)} - \mathcal{D}_{(AB)} \frac{\partial c_{(A)}}{\partial z} + \mathcal{D}_{(AB)} \frac{c_{(A)}}{c_{(B)}} \frac{\partial c_{(B)}}{\partial z} \tag{6}$$

In view of assumptions (i) and (iv), the molar flux of oxygen in both layers can be expressed as

$$\begin{aligned} N^{(o)}_{(O_2)} &= -\mathcal{D}^{(o)} \frac{\partial c^{(o)}_{(O_2)}}{\partial z} \\ N^{(m)}_{(O_2)} &= c^{(m)}_{(O_2)} v^{(m)}_{(met)} - \mathcal{D}^{(m)} \frac{\partial c^{(m)}_{(O_2)}}{\partial z} \end{aligned} \tag{7}$$

From assumption (iv) and the differential mass balance for the metal, we have

$$\frac{\partial v^{(m)}_{(met)}}{\partial z} = 0 \tag{8}$$

Using Eqs. (7) and (8), we can write Eqs. (1) and (2) as

$$\frac{\partial c^{(o)}_{(O_2)}}{\partial t} = \mathcal{D}^{(o)} \frac{\partial^2 c^{(o)}_{(O_2)}}{\partial z^2}, \quad 0 < z < h(t) \tag{9}$$

$$\frac{\partial c^{(m)}_{(O_2)}}{\partial t} + v^{(m)}_{(met)} \frac{\partial c^{(m)}_{(O_2)}}{\partial z} = \mathcal{D}^{(m)} \frac{\partial^2 c^{(m)}_{(O_2)}}{\partial z^2}, \quad h(t) < z < s(t) \tag{10}$$

in which the diffusion coefficients are considered to be constant by assumption (vii).

At each point on the metal–oxide interface, the jump mass balances [16] for metal, oxide and $O_2$ require

$$c^{(m)}_{(met)} \left(v^{(m)}_{(met)} - u\right) = r^{(\sigma)}_{(met)} \tag{11}$$

$$c^{(o)}_{(ox)} u = r^{(\sigma)}_{(ox)} \tag{12}$$

$$c^{(m)}_{(O_2)} \left(v^{(m)}_{(O_2)} - u\right) - c^{(o)}_{(O_2)} \left(v^{(o)}_{(O_2)} - u\right) = r^{(\sigma)}_{(O_2)} \tag{13}$$

Here $u$ is the speed of displacement of the metal–oxide interface and $r^{(\sigma)}_{(A)}$ is the rate of production of species $A$ per unit area on the phase interface.

In analyzing this problem the oxidation at the metal–oxide interface

$$a\,\text{metal} + O_2 \rightarrow b\,\text{oxide} \tag{14}$$

is assumed to be a simple first-order reaction with respect to oxygen. Thus

$$r^{(\sigma)}_{(O_2)} = \frac{r^{(\sigma)}_{(met)}}{a} = -\frac{r^{(\sigma)}_{(ox)}}{b} = -kc^{(o)}_{(O_2)} \tag{15}$$

where $k$ is a reaction rate coefficient for the oxidation. Recognizing this, we can eliminate $r^{(\sigma)}_{(met)}$ among Eqs. (11)–(13) to obtain

$$\text{at } z = h: \quad u = \frac{b\gamma(N^{(o)}_{(O_2)} - N^{(m)}_{(O_2)})}{c^{(m)}_{(met)} + b\gamma(c^{(o)}_{(O_2)} - c^{(m)}_{(O_2)})} \tag{16}$$

and

$$\text{at } z = h: \quad v^{(m)}_{(met)} = \left(1 - \frac{a}{b\gamma}\right) u \tag{17}$$

Here we have introduced the Pilling–Bedworth ratio defined as

$$\gamma \equiv \frac{c^{(m)}_{(met)}}{c^{(o)}_{(ox)}} \tag{18}$$

From Eqs. (7), (16) and (17), we have

$$\text{at } z = h: \quad u = \frac{dh}{dt} = \frac{b\gamma}{c^{(m)}_{(met)}\epsilon}\left(\mathcal{D}^{(m)}\frac{\partial c^{(m)}_{(O_2)}}{\partial z} - \mathcal{D}^{(o)}\frac{\partial c^{(o)}_{(O_2)}}{\partial z}\right) \tag{19}$$

and

$$\text{at } z = h: \quad v^{(m)}_{(met)} = \frac{b\gamma - a}{c^{(m)}_{(met)}\epsilon}\left(\mathcal{D}^{(m)}\frac{\partial c^{(m)}_{(O_2)}}{\partial z} - \mathcal{D}^{(o)}\frac{\partial c^{(o)}_{(O_2)}}{\partial z}\right) \tag{20}$$

where

$$\epsilon \equiv 1 + \left.\frac{b\gamma c^{(o)}_{(O_2)} - a c^{(m)}_{(O_2)}}{c^{(m)}_{(met)}}\right|_{z=h} \tag{21}$$

Using Eqs. (8) and (20), we have

$$v^{(m)}_{(met)} = \frac{b\gamma - a}{c^{(m)}_{(met)}\epsilon}\left(\mathcal{D}^{(m)}\left.\frac{\partial c^{(m)}_{(O_2)}}{\partial z}\right|_{z=h} - \mathcal{D}^{(o)}\left.\frac{\partial c^{(o)}_{(O_2)}}{\partial z}\right|_{z=h}\right) \tag{22}$$

This allows Eq. (10) to take the forms

$$\frac{\partial c^{(m)}_{(O_2)}}{\partial t} + \frac{b\gamma - a}{c^{(m)}_{(met)}\epsilon}\left(\mathcal{D}^{(m)}\left.\frac{\partial c^{(m)}_{(O_2)}}{\partial z}\right|_{z=h} - \mathcal{D}^{(o)}\left.\frac{\partial c^{(o)}_{(O_2)}}{\partial z}\right|_{z=h}\right)\frac{\partial c^{(m)}_{(O_2)}}{\partial z} = \mathcal{D}^{(m)}\frac{\partial^2 c^{(m)}_{(O_2)}}{\partial z^2}, \quad h(t) < z < s(t) \tag{23}$$

The initial condition is

$$\text{at } t = 0: \quad c^{(m)}_{(O_2)} = 0 \tag{24}$$

from assumption (ii).

In view of assumption (iii), we also have

$$\text{at } z = 0: \quad c^{(o)}_{(O_2)} = c_{eq} \tag{25}$$

Eq. (12) becomes in view of Eqs. (15) and (19)

$$\text{at } z = h: \quad \mathcal{D}^{(m)}\frac{\partial c^{(m)}_{(O_2)}}{\partial z} - \mathcal{D}^{(o)}\frac{\partial c^{(o)}_{(O_2)}}{\partial z} = k\epsilon c^{(o)}_{(O_2)} \tag{26}$$

There exists a solubility limit $c_s$ of oxygen in the metal, which is a function of temperature [3,8,17,18]. We will assume that the solubility limit is quickly achieved at the metal–oxide interface during a high temperature oxidation [3],

$$\text{at } z = h: \quad c^{(m)}_{(O_2)} = c_s \tag{27}$$

Very far away from the metal–oxide interface, the concentration of oxygen is assumed to keep the initial state:

$$\text{as } z \to s: \quad c^{(\mathrm{m})}_{(\mathrm{O}_2)} \to 0 \tag{28}$$

For simplicity, let us introduce the following dimensionless variables

$$c^{(\mathrm{m})\star} \equiv \frac{c^{(\mathrm{m})}_{(\mathrm{O}_2)}}{c_{\mathrm{eq}}}, \quad c^{(\mathrm{o})\star} \equiv \frac{c^{(\mathrm{o})}_{(\mathrm{O}_2)}}{c_{\mathrm{eq}}}, \quad t^\star \equiv t\frac{\mathcal{D}^{(\mathrm{o})}}{{s_0}^2}, \quad k^\star = k\frac{s_0}{\mathcal{D}^{(\mathrm{o})}}, \quad z^\star \equiv \frac{z}{s_0}, \quad h^\star \equiv \frac{h}{s_0}, \quad s^\star \equiv \frac{s}{s_0} \tag{29}$$

where $s_0$ is the initial thickness of the metal. In term of these dimensionless variables, Eqs. (9), (23)– (28) can be expressed by

$$\frac{\partial c^{(\mathrm{o})\star}}{\partial t^\star} = \frac{\partial^2 c^{(\mathrm{o})\star}}{\partial {z^\star}^2}, \quad 0 < z^\star < h^\star \tag{30}$$

$$\frac{1}{\alpha}\frac{\partial c^{(\mathrm{m})\star}}{\partial t^\star} + \frac{b\gamma - a}{\epsilon}\frac{c_{\mathrm{eq}}}{c^{(\mathrm{m})}_{(\mathrm{met})}}\left(\left.\frac{\partial c^{(\mathrm{m})\star}}{\partial z^\star}\right|_{z^\star=h^\star} - \frac{1}{\alpha}\left.\frac{\partial c^{(\mathrm{o})\star}}{\partial z^\star}\right|_{z^\star=h^\star}\right)\frac{\partial c^{(\mathrm{m})\star}}{\partial z^\star} = \frac{\partial^2 c^{(\mathrm{m})\star}}{\partial {z^\star}^2}, \quad h^\star < z^\star < s^\star \tag{31}$$

and

$$\text{at } t^\star = 0: \quad c^{(\mathrm{m})\star} = 0 \tag{32}$$

$$\text{at } z^\star = 0: \quad c^{(\mathrm{o})\star} = 1 \tag{33}$$

$$\text{at } z^\star = h^\star: \quad \alpha\frac{\partial c^{(\mathrm{m})\star}}{\partial z^\star} - \frac{\partial c^{(\mathrm{o})\star}}{\partial z^\star} = k^\star\epsilon c^{(\mathrm{o})\star} \tag{34}$$

$$\text{at } z^\star = h^\star: \quad c^{(\mathrm{m})\star} = {c_s}^\star \tag{35}$$

$$\text{at } z^\star \to s^\star: \quad c^{(\mathrm{m})\star} \to 0 \tag{36}$$

where

$$\alpha \equiv \frac{\mathcal{D}^{(\mathrm{m})}}{\mathcal{D}^{(\mathrm{o})}} \tag{37}$$

For the oxide layer, Eq. (30) is to be solved consistent with Eqs. (33) and (34); for the metal, Eq. (31) is to be solved consistent with Eqs. (32), (35) and (36).

In order to determine the position $h^\star$ of the metal–oxide boundary as a function of time, we will solve (19)

$$\frac{\mathrm{d}h^\star}{\mathrm{d}t^\star} = \frac{b\gamma}{\epsilon}\frac{c_{\mathrm{eq}}}{c^{(\mathrm{m})}_{(\mathrm{met})}}\left(\alpha\left.\frac{\partial c^{(\mathrm{m})\star}}{\partial z^\star}\right|_{z^\star=h^\star} - \left.\frac{\partial c^{(\mathrm{o})\star}}{\partial z^\star}\right|_{z^\star=h^\star}\right) \tag{38}$$

consistent with the initial condition

$$\text{at } t^\star = 0: \quad h^\star = 0 \tag{39}$$

This problem can be simplified by introducing the Landau transformation [13,15]:

$$\chi \equiv \frac{z^\star}{h^\star} \tag{40}$$

The Landau transformation was originally developed for describing the phase change of one-dimensional planar geometries by melting. It has been mainly applied to solve moving boundary problems [19–22].

By using the chain rule

$$\begin{aligned}
&\frac{\partial c^\star}{\partial z^\star} = \frac{1}{h^\star}\frac{\partial c^\star}{\partial \chi}\\
&\frac{\partial^2 c^\star}{\partial {z^\star}^2} = \frac{1}{{h^\star}^2}\frac{\partial^2 c^\star}{\partial \chi^2}\\
&\left.\frac{\partial c^\star}{\partial t^\star}\right|_{z^\star} = \frac{\partial c^\star}{\partial \chi}\frac{\partial \chi}{\partial t^\star} + \left.\frac{\partial c^\star}{\partial t^\star}\right|_{\chi} = \left\{-\frac{\chi}{h^\star}\frac{\partial c^\star}{\partial \chi} + \frac{\partial c^\star}{\partial h^\star}\right\}\frac{\mathrm{d}h^\star}{\mathrm{d}t^\star}
\end{aligned} \tag{41}$$

to transform from $c^\star(z^\star, t^\star)$ to $c^\star(\chi, h^\star)$, Eqs. (30) and (31) can be written

$$\frac{\phi b\gamma}{\epsilon}\left(h^\star\frac{\partial c^{(\mathrm{o})\star}}{\partial h^\star} - \chi\frac{\partial c^{(\mathrm{o})\star}}{\partial \chi}\right)\left\{\alpha\left.\frac{\partial c^{(\mathrm{m})\star}}{\partial \chi}\right|_{\chi=1} - \left.\frac{\partial c^{(\mathrm{o})\star}}{\partial \chi}\right|_{\chi=1}\right\} = \frac{\partial^2 c^{(\mathrm{o})\star}}{\partial \chi^2}, \quad 0 < \chi < 1 \tag{42}$$

and

$$\frac{\phi b\gamma}{\alpha\epsilon}\left[h^\star\frac{\partial c^{(\mathrm{m})\star}}{\partial h^\star}-\chi\frac{\partial c^{(\mathrm{m})\star}}{\partial\chi}+\left(1-\frac{a}{b\gamma}\right)\frac{\partial c^{(\mathrm{m})\star}}{\partial\chi}\right]\times\left\{\alpha\left.\frac{\partial c^{(\mathrm{m})\star}}{\partial\chi}\right|_{\chi=1}-\left.\frac{\partial c^{(\mathrm{o})\star}}{\partial\chi}\right|_{\chi=1}\right\}=\frac{\partial^2 c^{(\mathrm{m})\star}}{\partial\chi^2},\quad 1<\chi<S \tag{43}$$

The boundary conditions are now

$$\text{at } h^\star=0:\quad c^{(\mathrm{m})\star}=0 \tag{44}$$

$$\text{at } \chi=0:\quad c^{(\mathrm{o})\star}=1 \tag{45}$$

$$\text{at } \chi=1:\quad \alpha\frac{\partial c^{(\mathrm{m})\star}}{\partial\chi}-\frac{\partial c^{(\mathrm{o})\star}}{\partial\chi}=k^\star h^\star\epsilon\, c^{(\mathrm{o})\star} \tag{46}$$

$$\text{at } \chi=1:\quad c^{(\mathrm{m})\star}=c_s{}^\star \tag{47}$$

$$\text{at } \chi\to S\equiv\frac{s^\star}{h^\star}:\quad c^{(\mathrm{m})\star}\to 0 \tag{48}$$

Here we have used Eq. (38) in the form

$$\frac{\mathrm{d}h^\star}{\mathrm{d}t^\star}=\frac{b\gamma}{\epsilon}\frac{\phi}{h^\star}\left(\alpha\left.\frac{\partial c^{(\mathrm{m})\star}}{\partial\chi}\right|_{\chi=1}-\left.\frac{\partial c^{(\mathrm{o})\star}}{\partial\chi}\right|_{\chi=1}\right) \tag{49}$$

and we have introduced

$$\phi\equiv\frac{c_{\mathrm{eq}}}{c^{(\mathrm{m})}_{(\mathrm{met})}} \tag{50}$$

It should be noticed that $S$ is a function of $h^\star$. This will be explained in Section 3.2. Eqs. (42) and (43) are to be solved for $c^{(\mathrm{o})\star}$ and $c^{(\mathrm{m})\star}$ consistent with the boundary conditions (44)–(48) as functions of $h^\star$ and $\chi$. Finally (49) can be used to determine $h^\star$ consistent with (39).

### 3.1. Perturbation analysis

In most practical cases $c_{\mathrm{eq}}$ is much smaller than $c^{(\mathrm{m})}_{(\mathrm{met})}$, i.e. $\phi\ll 1$, which suggests that a regular perturbation analysis can be applied for solving Eqs. (42) and (43), using $\phi$ as the perturbation parameter,

$$c^{(\mathrm{o})\star}(\chi,h^\star)=c_0^{(\mathrm{o})}(\chi,h^\star)+\phi c_1^{(\mathrm{o})}(\chi,h^\star)+\phi^2 c_2^{(\mathrm{o})}(\chi,h^\star)+\cdots \tag{51}$$

$$c^{(\mathrm{m})\star}(\chi,h^\star)=c_0^{(\mathrm{m})}(\chi,h^\star)+\phi c_1^{(\mathrm{m})}(\chi,h^\star)+\phi^2 c_2^{(\mathrm{m})}(\chi,h^\star)+\cdots \tag{52}$$

These are substituted into Eqs. (42) and (43) and the terms are ordered by the powers of $\phi$. The result is a sequence of systems of equations for the zeroth-order solution $c_0$, for the first-order solution $c_1$ and for the second-order solution $c_2$, etc. For a small $\phi$, the first-order perturbation solution is enough to describe the concentration of oxygen.

#### 3.1.1. Zeroth-order perturbation

From Eqs. (43) and (52), the zeroth-order perturbation for the metal phase is

$$\frac{\partial^2 c_0^{(\mathrm{m})}}{\partial\chi^2}=0 \tag{53}$$

which should be solved consistent with the zeroth-order perturbation of (47) and (48)

$$\text{at } \chi=1:\quad c_0^{(\mathrm{m})}=c_s{}^\star \tag{54}$$

$$\text{at } \chi\to S:\quad c_0^{(\mathrm{m})}\to 0 \tag{55}$$

The solution of (53) consistent with (54) and (55) is

$$c_0^{(\mathrm{m})}=\frac{c_s{}^\star(S-\chi)}{S-1} \tag{56}$$

The zeroth-order perturbation for the oxide phase is obtained from (42) and (51)

$$\frac{\partial^2 c_0^{(\mathrm{o})}}{\partial\chi^2}=0 \tag{57}$$

Integrating this consistent with the zeroth-order perturbation of (45) and (46)

$$\text{at } \chi = 0: \quad c_0^{(o)} = 1 \tag{58}$$

$$\text{at } \chi = 1: \quad \alpha \frac{\partial c_0^{(m)}}{\partial \chi} - \frac{\partial c_0^{(o)}}{\partial \chi} = k^\star h^\star \epsilon c_0^{(o)} \tag{59}$$

gives

$$c_0^{(o)} = 1 - \chi \frac{\alpha c_s{}^\star + h^\star k^\star \epsilon (S-1)}{(1 + h^\star k^\star \epsilon)(S-1)} \tag{60}$$

Note that the zeroth-order solutions (56) and (60) represent the quasi-steady-state one which can be obtained from Eqs. (30) and (31) by discarding the time derivatives.

### 3.1.2. First-order perturbation

The first-order perturbation of (43) is

$$\frac{b\gamma}{\alpha\epsilon}\left[h^\star \frac{\partial c_0^{(m)}}{\partial h^\star} - \chi \frac{\partial c_0^{(m)}}{\partial \chi} + \left(1 - \frac{a}{b\gamma}\right)\frac{\partial c_0^{(m)}}{\partial \chi}\right]\left\{\alpha \left.\frac{\partial c_0^{(m)}}{\partial \chi}\right|_{\chi=1} - \left.\frac{\partial c_0^{(o)}}{\partial \chi}\right|_{\chi=1}\right\} = \frac{\partial^2 c_1^{(m)}}{\partial \chi^2} \tag{61}$$

The corresponding boundary conditions are the first-order perturbations of (47) and (48)

$$\text{at } \chi = 1: \quad c_1^{(m)} = 0 \tag{62}$$

$$\text{at } \chi = S: \quad c_1^{(m)} = 0 \tag{63}$$

Substituting Eqs. (56) and (60) into Eq. (61) and integrating twice, we find

$$c_1^{(m)}(\chi, h^\star) = \frac{h^\star k^\star c_s{}^\star (S-\chi)(\chi-1)(1-S+\alpha c_s{}^\star)}{6\alpha(1+h^\star k^\star \epsilon)(S-1)^3} \times \left\{(S-1)\left[3a + b\gamma(S-2+\chi)\right] + h^\star b\gamma(S-2+\chi)\frac{\mathrm{d}S}{\mathrm{d}h^\star}\right\} \tag{64}$$

The first-order perturbation of Eq. (42) is

$$\frac{b\gamma}{\epsilon}\left(h^\star \frac{\partial c_0^{(o)}}{\partial h^\star} - \chi \frac{\partial c_0^{(o)}}{\partial \chi}\right)\left\{\alpha \left.\frac{\partial c_0^{(m)}}{\partial \chi}\right|_{\chi=1} - \left.\frac{\partial c_0^{(o)}}{\partial \chi}\right|_{\chi=1}\right\} = \frac{\partial^2 c_1^{(o)}}{\partial \chi^2} \tag{65}$$

which is to be solved consistent with the first-order perturbation of Eqs. (45) and (46)

$$\text{at } \chi = 0: \quad c_1^{(o)} = 0 \tag{66}$$

$$\text{at } \chi = 1: \quad \alpha \frac{\partial c_1^{(m)}}{\partial \chi} - \frac{\partial c_1^{(o)}}{\partial \chi} = k^\star h^\star \epsilon c_1^{(o)} \tag{67}$$

Eqs. (65)–(67) are satisfied with

$$\begin{aligned} c_1^{(o)}(\chi, h^\star) = {} & \frac{h^\star k^\star \chi(1-S+\alpha c_s{}^\star)}{6(1+h^\star k^\star \epsilon)^4 (S-1)^2}\left\{3ac_s{}^\star(1+h^\star k^\star \epsilon)^2(S-1) + b\gamma\left[h^{\star 2}k^{\star 2}\epsilon^2(S-1)\{3-\chi^2+h^\star k^\star \epsilon(1-\chi^2)\}\right.\right. \\ & \left.\left. + c_s{}^\star\left((1+h^\star k^\star \epsilon)^2(S-1)^2 + \alpha(1+2h^\star k^\star \epsilon)\{3-\chi^2+h^\star k^\star \epsilon(1-\chi^2)\}\right)\right] \\ & + \frac{b\gamma c_s{}^\star h^\star (1+h^\star k^\star \epsilon)}{S-1}\left[(1+h^\star k^\star \epsilon)^2(S-1)^2 + \alpha\{3-\chi^2+h^\star k^\star \epsilon(1-\chi^2)\}\right]\frac{\mathrm{d}S}{\mathrm{d}h^\star}\Bigg\} \end{aligned} \tag{68}$$

## 3.2. Oxide thickness

In order to obtain the oxide thickness, Eqs. (51) and (52) are substituted into Eq. (49) and the terms are ordered by the powers of $\phi$:

$$\frac{\mathrm{d}h^\star}{\mathrm{d}t^\star} = \frac{b\gamma}{\epsilon}\frac{\phi}{h^\star}\left(\alpha \left.\frac{\partial c_0^{(m)}}{\partial \chi}\right|_{\chi=1} - \left.\frac{\partial c_0^{(o)}}{\partial \chi}\right|_{\chi=1} + \phi\left\{\alpha \left.\frac{\partial c_1^{(m)}}{\partial \chi}\right|_{\chi=1} - \left.\frac{\partial c_1^{(o)}}{\partial \chi}\right|_{\chi=1}\right\} + \cdots\right) \tag{69}$$

At this point, let us discuss on how $S$, defined in Eq. (48), depends on $h^\star$. Since there is no oxidation in the metal phase including at the boundary $s$, the velocity of the boundary $s$ is equal to the velocity of the metal in the metal phase in Eq. (22):

$$\frac{\mathrm{d}s}{\mathrm{d}t} = \frac{b\gamma - a}{c^{(\mathrm{m})}_{(\mathrm{met})}\epsilon}\left(\mathcal{D}^{(\mathrm{m})}\frac{\partial c^{(\mathrm{m})}_{(\mathrm{O}_2)}}{\partial z}\bigg|_{z=h} - \mathcal{D}^{(\mathrm{o})}\frac{\partial c^{(\mathrm{o})}_{(\mathrm{O}_2)}}{\partial z}\bigg|_{z=h}\right) \tag{70}$$

From Eqs. (19) and (70), we have

$$\frac{\mathrm{d}s}{\mathrm{d}h} = 1 - \frac{a}{b\gamma} \tag{71}$$

Thus

$$s = \left(1 - \frac{a}{b\gamma}\right)h + s_0 \tag{72}$$

With the help of Eqs. (29) and (48), Eq. (72) becomes

$$S = \left(1 - \frac{a}{b\,\gamma}\right) + \frac{1}{h^\star} \tag{73}$$

In view of Eqs. (56), (60), (64), (68) and (73), Eq. (69) becomes

$$\begin{aligned}\frac{\mathrm{d}h^\star}{\mathrm{d}t^\star} &= \phi\frac{b\gamma k^\star(ah^\star - b\gamma + \alpha {c_s}^\star h^\star b\gamma)}{(1 + h^\star k^\star\epsilon)(ah^\star - b\gamma)} + \phi^2\frac{b\gamma h^\star {k^\star}^2(ah^\star - b\gamma + \alpha {c_s}^\star h^\star b\gamma)}{3(1 + h^\star k^\star\epsilon)^4(ah^\star - b\,\gamma)^3}\\ &\quad\times\Big\{a\,{c_s}^\star[2a\,h^\star b\,\gamma - b^2\gamma^2 - a^2{h^\star}^2 + \alpha{h^\star}^2b^2\gamma^2] - \epsilon^2{h^\star}^2{k^\star}^2(ah^\star - b\gamma)^2(a{c_s}^\star + b\gamma)\\ &\quad+ \epsilon{c_s}^\star h^\star k[4a^2h^\star b\gamma - 2a^3{h^\star}^2 + 2ab^2\gamma^2(\alpha{h^\star}^2 - 1) - \alpha h^\star b^3\gamma^3]\Big\} + \cdots\end{aligned} \tag{74}$$

From this, we can obtain the oxide thickness with respect to time. In the limit of an instantaneous reaction as $k^\star \to \infty$ and ${c_s}^\star \to 0$, Eq. (74) reduces to

$$\frac{\mathrm{d}h^\star}{\mathrm{d}t^\star} = \frac{b\gamma\phi}{h^\star\epsilon}\left\{1 - \frac{b\,\gamma\,\phi}{3\epsilon} + \cdots\right\} \tag{75}$$

Integrating this yields

$${h^\star}^2 = \frac{2b\gamma\phi t^\star}{\epsilon}\left\{1 - \frac{b\gamma\phi}{3\epsilon} + \cdots\right\} \tag{76}$$

*3.2.1. $k^\star$ Dependence on oxide thickness*

In Fig. 2, the oxide thickness for five different values of $k^\star$ is plotted using Eq. (74). As an illustration, we have followed Lagoudas et al. [12] in choosing $a = b = 1$, $\gamma = 1.766$, $\phi = 0.133$, ${c_s}^\star = 0.2925$ and $\epsilon \approx 1$. We have also chosen $\alpha = 0.1$. At a small value of $k^\star$, corresponding to the oxidation controlled by the rate of reaction, the oxide thickness linearly increases regardless of the oxidation time. As $k^\star$ increases, the growth rate of the oxide is transformed from linear to parabolic at early stage of oxidation. For a large value of $k^\star$ describing the oxidation controlled by diffusion, the oxide growth can be represented by a fully parabolic function.

For titanium oxidation at high temperatures, a parabolic rate of oxidation has been observed by Kofstad et al. [23] and by Unnam et al. [3]. More recently, Imbrie and Lagoudas [6] have studied the oxidation of titanium for solid cylindrical specimens, as well as the oxidation of a plane. On the basis of their observations, the oxidation of titanium can be expected to be diffusion controlled.

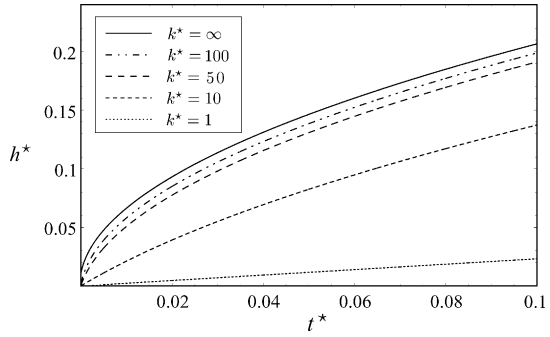


Fig. 2. Oxide thickness for five different values of $k^\star$ where $k^\star = ks_0/\mathcal{D}^{(\mathrm{o})}$.

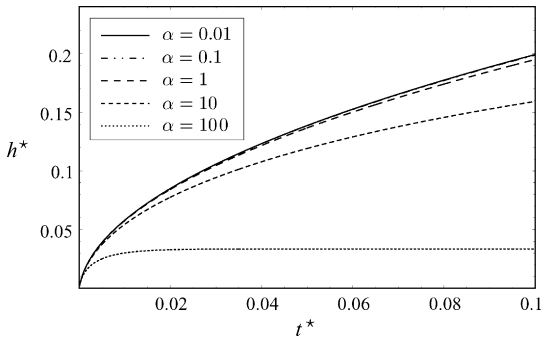


Fig. 3. Oxide thickness for five different values of $\alpha$ where $\alpha \equiv \mathcal{D}^{(m)}/\mathcal{D}^{(o)}$.

*3.2.2. $\alpha$ Dependence on oxide thickness*

Fig. 3 shows how the oxide thickness is affected by $\alpha$. The same parameters are used as in the previous section except that $\alpha$ is now varied and we arbitrarily choose $k^\star = 100$. As suggested in the previous section, we have chosen a relatively fast but not instantaneous reaction. Some of the oxygen diffusing to the interface from the oxide is not reacted, but it diffuses into the metal. As seen in Fig. 3, a relatively large value of $\alpha$ decreases the growth rate of oxide. In view of assumption (vi), as $\alpha$ increases, the concentration in the oxide at the interface decreases, and the reaction rate decreases. When $\alpha < 1$, the rate of reaction becomes controlled by the rate of diffusion of oxygen to the interface from the oxide.

*3.2.3. $\gamma$ Dependence on oxide thickness*

In Fig. 4, the oxide thickness for three different values of the Pilling–Bedworth ratio $\gamma$ is plotted using (74). The same parameters are used as in Section 3.2.1, again arbitrarily choosing $k^\star = 100$. As expected from (74), the growth rate of oxide is highly increased according to $\gamma$ increase.

*3.2.4. $c_s^\star$ Dependence on oxide thickness*

Unless the oxidation reaction is instantaneous, there occurs oxygen diffusion into the metal layer through the metal–oxide interface. Each metal has its own solubility of oxygen [3,17,18]. For the titanium oxidation, a wide range of oxygen solubility from 7 to 34 at.% has been reported [3,4,6–8,24]. It has been also observed that $c_s^\star$ varies with the exposure time and temperature [3,4]. Now the effect of $c_s^\star$ on the oxide thickness is shown in Fig. 5. As expected, a lower $c_s^\star$ gives rise to thicker oxide because a relatively large amount of oxygen involves in the oxidation reaction.

## 4. Comparing with experimental data

By comparing the oxide thickness and the concentration of oxygen predicted by our perturbation analysis with experimental data, we compute the diffusion coefficients of oxygen, as well as the reaction rate coefficient for the oxidation.

### *4.1. Silicon oxidation*

For silicon oxidation, there occurs no oxygen diffusion into the silicon substrate. The Pilling–Bedworth ratio $\gamma$ is 2.15 [5] and $\phi$ is generally of the order of $10^{-6}$ [15]. Fig. 6 compares the data of Lie et al. [25] for the growth of $SiO_2$ layer at five different

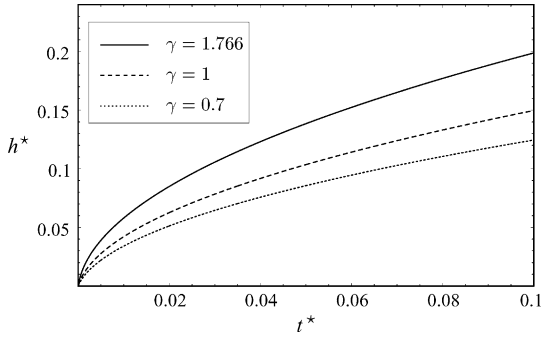


Fig. 4. Oxide thickness for three different values of $\gamma$.

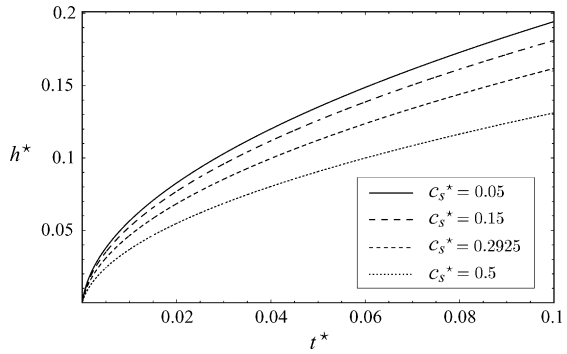


Fig. 5. Oxide thickness for four different values of $c_s^\star$ where $c_s^\star = c_s/c_{\text{eq}}$.

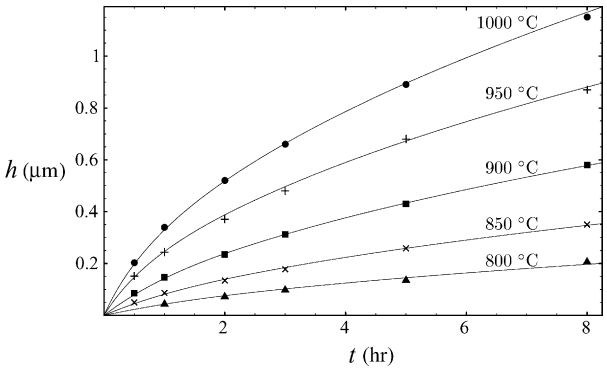


Fig. 6. Experimental data for the thickness $h$ (μm) of $SiO_2$ layer at $20.3 \times 10^5$ Pa and each temperature as a function of time $t$ (h). These are fitted to the thickness calculated by (74) to estimate the values of $k$ and $\mathcal{D}_{(O_2,SiO_2)}$.

temperatures with the oxide thickness predicted by (74). In this calculation we have used the same values of equilibrium concentration $c_{\text{eq}}$ as Peng et al. [26] used.

As seen in Fig. 6, the perturbation analysis gives a very good representation of the experimental data. In Table 1 the values of $k$ and $\mathcal{D}_{(O_2,SiO_2)}$ used in plotting Fig. 6 are listed.

Using a least-square fit to the data summarized in Table 1, we find

$$k = 9.69 \times 10^6 \exp\left(-\frac{E_a^k}{RT}\right) \tag{77}$$

and

$$\mathcal{D}_{(O_2,SiO_2)} = 2.73 \times 10^{-3} \exp\left(-\frac{E_a^D}{RT}\right) \tag{78}$$

where $E_a^k = 41.8$ kcal/mol and $E_a^D = 52.1$ kcal/mole, respectively. Under the assumption of instantaneous reaction, $k \to \infty$ at the $Si–SiO_2$ interface, Peng et al. [26] has obtained

$$\mathcal{D}_{(O_2,SiO_2)} = 5.05 \times 10^{-4} \exp\left(-\frac{54.8\,\text{kcal/mol}}{RT}\right) \tag{79}$$

### 4.2. Titanium oxidation

As mentioned in Section 3.2.4, oxygen can diffuse into titanium through the $Ti–TiO_2$ interface. Recently, Imbrie and Lagoudas [6] studied the oxidation of a flat titanium surface at 700 °C measuring both the oxide thickness as a function of time (Fig. 7) and the

Table 1
Estimated values of $k$ and $\mathcal{D}_{(O_2,SiO_2)}$ at five different temperatures

| | 800 °C | 850 °C | 900 °C | 950 °C | 1000 °C |
|---|---|---|---|---|---|
| $k$ (m/s) | 0.03 | 0.07 | 0.15 | 0.38 | 0.60 |
| $\mathcal{D}_{(O_2,SiO_2)}$ (μm²/s) | 0.06 | 0.2 | 0.6 | 1.4 | 2.7 |

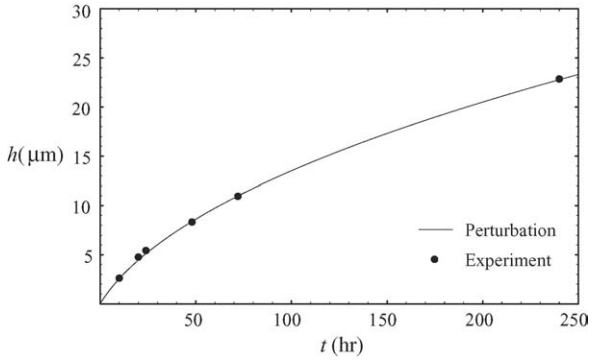


Fig. 7. The thickness $h$ of $TiO_2$ as a function of time $t$ measured by Imbrie and Lagoudas [6]. The curve is from (74).

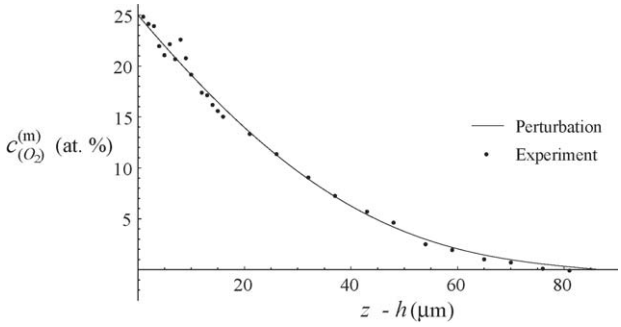


Fig. 8. Concentration of oxygen in the metal $c^{(m)}_{(O_2)}$ as a function of $z$–$h$ at 240 h as measured by Imbrie and Lagoudas [6]. The curve is from (52) using (56) and (64).

oxygen concentration in the metal phase at 240 h (Fig. 8). Our objective here is to determine the corresponding diffusion coefficients in the metal and oxide as well as the reaction rate coefficient.

From Imbrie and Lagoudas [6], we have the oxygen concentration at the metal–oxide interface is 25 at.%. We also know that Ti(O) varies linearly from 4.52 to 5.04 g/cm$^3$ as the oxygen concentration varies from 0 to 34 at.% [27]. This allows us to compute $c_s = 15.3\,\text{kmol/m}^3$. Imbrie and Lagoudas [6] also measured $c_{\text{eq}} = 17.7\,\text{kmol/m}^3$, $\gamma = 1.779$ and $s_0 = 100\,\mu\text{m}$. We have used that $c_{(\text{Ti})} = 94.4\,\text{kmol/m}^3$ [28].

We will compare (74) with the experimental measurements of $h$ as a function of $t$ as shown in Fig. 7. We also wish to compare (52) using (56) and (64) with the experimental measurement of $c^{(m)}_{(O_2)}$ of $z$–$h$ in Fig. 8. In these comparisons, there are three unknown parameters: $k^\star$, $\alpha$, and $\mathcal{D}_{(O_2,TiO_2)}$. These parameters were determined by a least-squares fit of (74) and (52) to these two experimental curves: $k^\star = 20$, $\mathcal{D}_{(O_2,TiO_2)} = 1.32 \times 10^{-3}\,\mu\text{m}^2/\text{s}$ and $\alpha = 0.12$, i.e., $\mathcal{D}_{(O_2,Ti)} = 1.58 \times 10^{-4}\,\mu\text{m}^2/\text{s}$. Under the assumption that oxygen concentration was assumed to be linearly distributed within the oxide, Unnam et al. [3] obtained $\mathcal{D}_{(O_2,TiO_2)} = 2.91 \times 10^{-2}\,\mu\text{m}^2/\text{s}$, and $\mathcal{D}_{(O_2,Ti)} = 5.76 \times 10^{-4}\,\mu\text{m}^2/\text{s}$. While Entchev et al. [28] have reported $\mathcal{D}_{(O_2,TiO_2)} = 1.34 \times 10^{-3}\,\mu\text{m}^2/\text{s}$, which was calculated by using the assumptions that the oxidation reaction is instantaneous at the Ti–$TiO_2$ interface, and that there occurs no oxygen diffusion into titanium.

## 5. Conclusions

For the oxidation of a metal with oxygen diffusion through the oxide and metal, we have employed a perturbation analysis, where the perturbation parameter $\phi$ is the ratio of the molar density of oxygen in the oxide at the oxide–oxygen interface to the molar density of metal. We have avoided the assumptions made in previous papers [2,4,3,12,28], such as the oxygen concentration being linearly distributed in the oxide, no volumetric expansion during the oxidation, or instantaneous reaction at the metal–oxide interface.

We have found an expression for the oxide growth rate and the oxygen concentration in the metal and oxide in which the reaction rate as well as the volume expansion are taken into account. The results were fit to the experimental data by Lie et al. [25] and Imbrie and Lagoudas [6], in order to determine the diffusion coefficients in the metal and in the oxide, as well as the reaction rate coefficient at the metal–oxide interface.

It has been shown that, when the oxidation is reaction-controlled, the oxide grows linearly and that, as the reaction rate increases, the oxide grows more parabolically. A fully parabolic growth rate indicates that the oxidation is diffusion-controlled. This forms an easy test by which one can decide whether the oxidation is reaction-controlled or diffusion-controlled.

The approach developed here is not limited to the oxidation of either silicon or titanium, but it may be extended to the oxidation of any metal where the oxidation reaction involves $O_2$ and occurs at the metal–oxide interface. It is only necessary to properly recognize the stoichiometry of the oxidation reaction (14).

## References

[1] C. Wagner, On the solution of diffusion problems involving concentration-dependent diffusion coefficients, J. Met. 4 (1951) 91–96.
[2] P. Kofstad, High Temperature Oxidation of Metals, Wiley, New York, 1966.
[3] J. Unnam, R.N. Shenoy, R.K. Clark, Oxidation of commercial purity titanium, Oxid. Met. 26 (3) (1986) 231–252.
[4] R.N. Shenoy, J. Unnam, R.K. Clark, Oxidation and embrittlement of Ti–6Al–2Sn–4Zr–2Mo alloy, Oxid. Met. 26 (1–2) (1986) 105–124.
[5] H.E. Evans, Stress effects in high temperature oxidation of metals, Int. Mater. Rev. 40 (1) (1995) 1–39.
[6] P.K. Imbrie, D.C. Lagoudas, The morphological evolution of $TiO_2$ scale formed on various 1-d and 2-d geometries of titanium, Oxid. Met. 55 (3–4) (2001) 359–399.
[7] A. Jenkins, The oxidation of titanium at high temperatures in an atmosphere of pure oxygen, J. Inst. Met. 82 (1953) 213–221.
[8] P. Kofstad, P. Anderson, O. Krudtaa, Oxidation of titanium in the temperature range 800–1200 °C, J. Less-Common Met. 3 (1961) 89–97.
[9] N.B. Pilling, R.E. Bedworth, The oxidation of metals at high temperature, J. Inst. Met. 29 (1923) 529–582.
[10] J. Crank, The Mathematics of Diffusion, Clarendon Press, Oxford, 1975.
[11] J. Crank, Free and Moving Boundary Problems, Clarendon Press, Oxford, 1984.
[12] D.C. Lagoudas, X. Ma, D.A. Miller, D.H. Allen, Modeling of oxidation in metal matrix composites, Int. J. Eng. Sci. 33 (15) (1995) 2327–2343.
[13] H.G. Landau, Heat conduction in a melting solid, Quart. Appl. Math. 8 (1950) 81–94.
[14] J.D. Cole, Perturbation Methods in Applied Mathematics, Blaisedell, New York, 1972.
[15] V.R. Mhetar, L.A. Archer, A perturbation solution for the interfacial oxidation of silicon, J. Vac. Sci. Technol. B 16 (4) (1998) 2121–2124.
[16] J.C. Slattery, Advanced Transport Phenomena, first ed., Cambridge University Press, Cambridge, 1999.
[17] R.J. Wasilewski, The solubility of oxygen in, and the oxides of, tantalum, J. Am. Chem. Soc. 75 (1953) 1001–1002.
[18] R.P. Elliott, Constitution of Binary Alloys, First Supplement, McGraw-Hill, New York, 1965.
[19] A.A. Elbahadli, R.M. Hassan, Melting in a rectangular enclosure—variational approach, JSME Int. J. Series I-Solid Mech. Strength Mater. 35 (2) (1992) 210–215.
[20] B.F. Blackwell, R.E. Hogan, One-dimensional ablation using Landau transformation and finite control volume procedure, J. Thermophys. Heat Transfer 8 (2) (1994) 282–287.
[21] S. Sundarraj, V.R. Voller, The binary alloy problem in an expanding domain:the microsegregation problem, Int. J. Heat Mass Transfer 36 (3) (1993) 713–723.
[22] J.P. Hsu, S.W. Huang, S. Tseng, Mathematical simulation of soft baking in photoresist processing, J. Electrochem. Soc. 147 (5) (2000) 1920–1924.
[23] P. Kofstad, K. Hauffe, H. Kjollesdal, Investigation on the oxidation mechanism of titanium, Acta Chem. Scand. 12 (1958) 239–266.
[24] T. Hurlen, Defect structure of rutile, Acta Chem. Scand. 13 (1959) 365–376.
[25] L.N. Lie, R.R. Razouk, B.E. Deal, High pressure oxidation of silicon in dry oxygen, J. Electrochem. Soc. 129 (12) (1982) 2828–2834.
[26] K.Y. Peng, L.C. Wang, J.C. Slattery, A new theory for silicon oxidation, J. Vac. Sci. Technol. B 14 (5) (1996) 3316–3320.
[27] S. Andersson, B. Collen, U. Kuylenstierna, Phase analysis studies on the titanium-oxygen system, Acta Chem. Scand. 11 (1957) 1641–1652.
[28] P.B. Entchev, D.C. Lagoudas, J.C. Slattery, Effects of non-planar geometries and volumetric expansion in the modeling of oxidation in titanium, Int. J. Eng. Sci. 39 (2001) 695–714.